Shock and Vibration 15 (2008) 481–492
IOS Press

Vibration analysis of circular arch element using curvature

H. Saffari[a], R. Tabatabaei[a,*] and S.H. Mansouri[b]
[a]*Civil Engineering Department, University of Kerman, Kerman, Iran*
[b]*Mechanical Engineering Department, University of Kerman, Kerman, Iran*

Received 20 July 2006
Revised 22 February 2007

Abstract. In this paper, a finite element technique was used to determine the natural frequencies, and the mode shapes of a circular arch element was based on the curvature, which can fully represent the bending energy and by the equilibrium equations, the shear and axial strain energy were incorporated into the formulation. The treatment of general boundary conditions dose need a consideration when the element is incorporated by the curvature-based formula. This can be obtained by the introduction of a transformation matrix between nodal curvatures and nodal displacements. The equation of the motion for the element was obtained by the Lagrangian equation. Four examples are presented in order to verify the element formulation and its analytical capability.

Keywords: Circular arch element, curvature, free vibration, natural frequencies, membrane-shear locking

1. Introduction

The study of free vibration is an important prerequisite for all dynamic response calculations for elastic systems. The natural frequencies and mode shapes can be obtained by free vibration analysis. The equations of motion for an elastic system with a finite number of degrees of freedom were derived through the application of the virtual-work principle for dynamic loading [19].

The most important subject discussed in this article is the vibration analysis of curved beams in the design of the structural components and the machine elements by using the finite element method. The development of finite elements for a curved beam has received considerable attention in recent years. A curved beam may can be modeled by some straight beam elements and one can use the different finite element models to analyze the thin arch structures [4]. The models, varied in the polynomial orders, were used to interpolate displacement components. Choosing the three different combinations of shape function [2], carried out a static analysis of beams for the lateral and in-plane displacements [17]. used four different shape functions for the vibration curved beam problems [3]. used a mixed trigonometric polynomial displacement field derived from an assumed constant membrane strain and linear curvature strain field. Based on Timoshenko beam theory [7] derived trigonometric basis functions for curved beam element. A coupled polynomial displacement field has been presented by [15,16]. Besides the displacement field [9,10], introduced an additional degree of freedom, which was the nodal shear strain. The analysis of curved beams derived by [14], included the effects of shear deformation and rotatory inertia. The same equation was given by [1] without the considering of the effects of shear deformation [8]. gave a theory about analysis of thin-walled curved box beam [12]. used several Fourier P-elements for the in-plane vibration of the thin and thick curved beam. Much of the attention has been focused to compensate the locking phenomena over the years since the locking

*Corresponding author. Tel.: +98 9133429226; Fax.: +98 341 3211497; E-mail: SRAMIN47@yahoo.com.

ISSN 1070-9622/08/$17.00

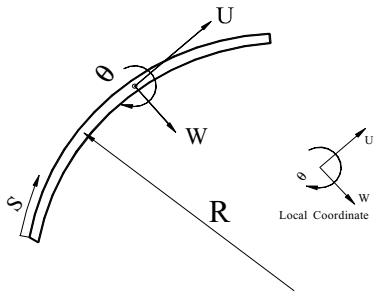

Fig. 1. Components of displacement in a typical curved beam.

concept was first introduced by improved numerical integration methods. These approaches are mostly in use, but it cannot represent the curvature of curved beam completely; therefore, following the method of [11], the present authors such as [18] used the formulation of a curved beam element with six nodes for curvature to compensate for the undesirable shear or axial locking phenomenon completely. The formulation is capable of representing the behavior of the curved beam with adequate accuracy and efficiency as compared to previous methods.

In the present work, a new formulation for vibration analysis of a circular arch element with three nodes for curvature is presented. This formulation focuses on four major differences between the present study and the others method. One of the four major differences is that the nodal parameters are not pure displacements, but the curvatures in three nodes elements. Here, we use three nodes for curvature because components of mass matrix are derived easier than six nodes. Another differences is that in order to avoid membrane and shear locking phenomena, the shear and tangential strains are incorporated into the total potential energy by the force equilibrium equation. The membrane locking occurs due to the fact that the element cannot bend without being stretched and shear locking takes place, because when the elements are subject to bending moments alone, the conventional lower-order elements are unable to represent the condition of zero radial shear strains. Another major differences is that the total mass matrix includes the effects of shear deformation and rotatory inertia. The final difference has an interesting point in this new formulation and that is the way it can easily be used to model curved beams and to analyze the free vibration problems. Incorporating these aspects into the new formulation resulted in a more efficient and less problematic curved beam element. For this task, the radial and tangential displacements and sectional rotation are obtained by integrating the assumed curvature filed. The treatment of general boundary conditions does need the consideration when the element employs the curvature-based formulation. This can be obtained by introduction of a transformation matrix between nodal curvature and nodal displacements. The transformed matrix is obtained by eliminating the components of the rigid body motion that is embedded in the two nodal displacements of typical circular arch element. The final finite element equilibrium equation is written in terms of the displacement components of the two-edge nodes only. The equation of motion for the element is obtained by the Lagrangian for dynamic loading. The formulation will be applied to four types of problems to verify the concept employed and its numerical results are given in tabular form that are compared with the known results obtained in other approaches.

2. General equations of arch element in the polar coordinates

The circular arch element with the radius of curvature R and arclength L loaded in plane is shown in Fig. 1. The radial displacement, W, the tangential displacement, U, and the rotation, θ, are also shown in this figure. These components are related to the curvature κ, the shearing strain γ, and the tangential strain ε, respectively by:

$$\kappa = \frac{\partial \theta}{\partial S}, \quad \gamma = \frac{\partial W}{\partial S} - \theta + \frac{U}{R}, \quad \varepsilon = \frac{\partial U}{\partial S} - \frac{W}{R} \tag{1}$$

The bending moment, M_b, the shearing force, V_b, and the axial force, N, are also related to the components of strain:

$$M_b = EI\kappa, \quad V_b = nGA\gamma, \quad N = EA\varepsilon \tag{2}$$

The equilibrium conditions of a small element in a circular arch takes the final form:

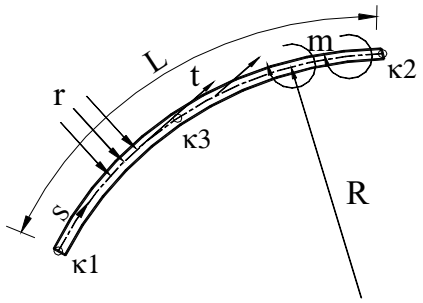

Fig. 2. Nodal curvatures and applied loads in a 3-node circular arch element.

$$\frac{\partial M_b}{\partial S} + V_b = 0, \quad \frac{\partial V_b}{\partial S} + \frac{N}{R} = 0 \tag{3}$$

Using the Eqs (2), (3) shearing and the axial strains can be expressed in terms of the curvature κ, by

$$\varepsilon = \frac{IR}{A} \cdot \left(\frac{1}{\frac{\partial S^2}{\partial^2 \kappa}} \right), \quad \gamma = -\frac{EI}{GAn} \cdot \frac{1}{\frac{\partial S}{\partial \kappa}} \tag{4}$$

To determine θ, W and U, we substitute the Eq. (4) in Eq. (1) and the relationship between the rotation θ and curvature κ obtained from Eq. (1) as:

$$\theta = \int_0^S \kappa dS + C_\theta \tag{5}$$

Where C_θ is the constant of integration. The radial displacement is determined by the following equation, which results from Eqs (1–4):

$$\frac{\partial W^2}{\partial S^2} + \frac{1}{R^2} \cdot W = \kappa - \left(\frac{EI}{GAn} + \frac{I}{A} \right) \cdot \frac{1}{\frac{\partial S^2}{\partial^2 \kappa}} \tag{6}$$

The solution for W consists of the homogeneous and particular parts. The homogeneous solution has sinusial terms and two integration constants; the particular solution is a function of the curvature since there appear κ and $\frac{1}{\frac{\partial S^2}{\partial^2 \kappa}}$ on the right-hand side of the Eq. (6):

$$W = (W^h + W^P), \quad W^h = C_{W1} \cdot \mathrm{Cos}\frac{S}{R} + C_{W2} \cdot \mathrm{Sin}\frac{S}{R}, \quad W^P = W^P(\kappa) \tag{7}$$

The three constant appearing in the Eqs (5) and (7) shows the components of rigid-body motion of the curved element. Finally, the tangential displacement is determined by the results of the Eqs (1–4):

$$U = R \cdot \left(\theta - \frac{\partial W}{\partial S} - \frac{EI}{GAn} \cdot \frac{1}{\frac{\partial S}{\partial \kappa}} \right) \tag{8}$$

2.1. Interpolation of curvature κ, and other components of the displacement

Now, the interpolation process for curvature is to be carried on. It is worth noting here before the formulation that curvature should be interpolated with the order equal or higher than 2. A 3-node element for the curvature since the polynomial functions for the interpolation of the curvature with the order equal to two is presented in this paper. When the curvature in the element is interpolated as shown in Fig. 2, the following equations holds:

$$\kappa = \{H_\kappa\} \cdot \{V\}, \quad \{V\} = [\kappa_1, \kappa_2, \kappa_3]^T, \quad \{H_\kappa\} = [h_1^\kappa, h_2^\kappa, h_3^\kappa] \tag{9}$$

$$h_1^\kappa = 1 - 3\frac{S}{L} + 2\left(\frac{S}{L}\right)^2, h_2^\kappa = -\frac{S}{L} + 2\left(\frac{S}{L}\right)^2, h_3^\kappa = 4\frac{S}{L} - 4\left(\frac{S}{L}\right)^2 \tag{10}$$

Equation (9) in Eq. (5) gives the sectional rotation as:

$$\theta = \{H_\theta\} \cdot \{V\} + C_\theta, \quad \{H_\theta\} = [h_1^\theta, h_2^\theta, h_3^\theta] \tag{11}$$

Also the radial displacement is given by Eq. (9) in Eq. (7) as shown below:

$$W = \{H_{WP}\} \cdot \{V\} + C_{W1} \cdot \mathrm{Cos}\frac{S}{R} + C_{W2} \cdot \mathrm{Sin}\frac{S}{R}, \quad \{H_{WP}\} = [h_1^{WP}, h_2^{WP}, h_3^{WP}] \tag{12}$$

Finally, the tangential displacement is written by Eq. (8) as shown below:

$$U = \{H_U\} \cdot \{V\} + R \cdot \{C_\theta\} + C_{W1} \cdot \mathrm{Sin}\frac{S}{R} - C_{W2} \cdot \mathrm{Cos}\frac{S}{R}, \quad \{H_U\} = [h_1^U, h_2^U, h_3^U] \tag{13}$$

2.2. Transformation matrix between nodal curvatures and nodal displacements

When nodal curvatures (V) are used for the interpolation, it is not easy to use the boundary conditions given as displacements. Therefore, we must consider a circular arch element with two nodal displacements in which the six boundary conditions are given at the nodes of the element as shows in Fig. 3. When the components of rigid-body motion embedded in each nodal displacement are eliminated, the relations between nodal displacements (Δ), and nodal curvatures can be found by using the following Eqs (11–13). Note that the three constants C_θ, $C_{W1}$and C_{W2} appearing in the equations represent the rigid-body motion components. With the components of the rigid-body motion eliminated [19]:

$$\theta_1 = \{H_\theta|_0\} \cdot \{V\} + C_\theta = C_\theta \tag{14}$$

$$W_1 = \{H_{WP}|_0\} \cdot \{V\} + C_{W1} \tag{15}$$

$$U_1 = \{H_U|_0\} \cdot \{V\} + R \cdot C_\theta - C_{W2} \tag{16}$$

$$\theta_2 = \{H_\theta|_L\} \cdot \{V\} + C_\theta \tag{17}$$

$$W_2 = \{H_{WP}|_L\} \cdot \{V\} + C_{W1} \cdot \mathrm{Cos}\frac{L}{R} + C_{W2} \cdot \mathrm{Sin}\frac{L}{R} \tag{18}$$

$$U_2 = \{H_U|_L\} \cdot \{V\} + R \cdot C_\theta + C_{W1} \cdot \mathrm{Sin}\frac{L}{R} - C_{W2} \cdot \mathrm{Cos}\frac{L}{R} \tag{19}$$

or in the matrix form relationship between the nodal curvatures and nodal displacements can be obtained by:

$$[T_\kappa] \cdot \{V\} = [T_U] \cdot \{\Delta\} \tag{20}$$

where

$$\{\Delta\} = [W_1, U_1, \theta_1, W_2, U_2, \theta_2]^T \tag{21}$$

and

$$[T_\kappa] = \begin{bmatrix} H_{WP}|_L \cdot V - H_{WP}|_0 \mathrm{Cos}\frac{L}{R} + H_U|_0 \mathrm{Sin}\frac{L}{R} \\ H_U|_L \cdot V - H_{WP}|_0 \mathrm{Sin}\frac{L}{R} - H_U|_0 \mathrm{Cos}\frac{L}{R} \\ H_{\theta|_L} \end{bmatrix} \tag{22}$$

$$[T_U] = \begin{bmatrix} -\mathrm{Cos}\frac{L}{R} & \mathrm{Sin}\frac{L}{R} & -R \cdot \mathrm{Sin}\frac{L}{R} & 1 & 0 & 0 \\ -\mathrm{Sin}\frac{L}{R} & -\mathrm{Cos}\frac{L}{R} & -R \cdot (1 - \mathrm{Cos}\frac{L}{R}) & 0 & 1 & 0 \\ 0 & 0 & -1 & 0 & 0 & 1 \end{bmatrix} \tag{23}$$

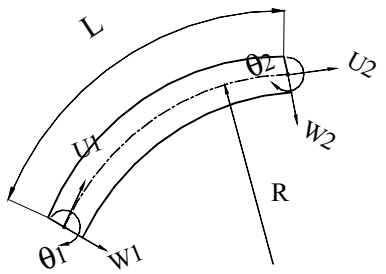

Fig. 3. Nodal displacement at 3-node circular arch element.

The transformation matrix, which relates the curvature vector at the three nodes and the displacement vector at two-nodes as shown in Fig. 3 can be expressed as follows:

$$\{V\} = [T] \cdot \{\Delta\} \tag{24}$$

$$[T] = [T_k^{-1}] \cdot [T_U] \tag{25}$$

For static problems the total displacements Q in the continuous element as Fig. 3 can be related to a finite number of displacements selected at two nodes in boundary conditions. This relationship is expressed by a column matrix of $[f]$ as:

$$[Q] = [f] \cdot \{\Delta\}, \quad [Q] = [W\ U\ \theta] \tag{26}$$

and $[f]$ is the shape function matrix. By using the Eqs (20–25), components of matrix $[f]$ we get:

$$[f] = [f_W\ f_U\ f_\theta]^T \tag{27}$$

where

$$\{f_W\} = \left(\{H_{WP}\} - \{H_{WP}|_0\} \cdot \mathrm{Cos}\frac{S}{R} + \{H_U|_0\} \cdot \mathrm{Sin}\frac{S}{R}\right) \cdot [T] + \{H_{W0}\} \tag{28}$$

$$\{H_{W0}\} = \left[\mathrm{Cos}\frac{S}{R} - \mathrm{Sin}\frac{S}{R}\ \ R \cdot \mathrm{Sin}\frac{S}{R} 0\ \ 0\ \ 0\right] \tag{29}$$

$$\{f_U\} = \left(\{H_U\} - \{H_{WP}|_0\} \cdot \mathrm{Sin}\frac{S}{R} - \{H_U|_0\} \cdot \mathrm{Cos}\frac{S}{R}\right) \cdot [T] + \{H_{U0}\} \tag{30}$$

$$\{H_{U0}\} = \left[\mathrm{Sin}\frac{S}{R}\ \ \mathrm{Cos}\frac{S}{R}\ \ R \cdot \left(1 - \mathrm{Cos}\ \frac{S}{R}\right)\ \ 0\ \ 0\ \ 0\right] \tag{31}$$

$$\{f_\theta\} = \{H_\theta\} \cdot [T] + \{H_{\theta 0}\} \tag{32}$$

$$\{H_{\theta 0}\} = \begin{bmatrix} 0 & 0 & 1 & 0 & 0 & 0 \end{bmatrix} \tag{33}$$

Other components of the displacement can be obtained in terms of the nodal displacement vector and transformation matrix above. The radial displacement W as shown in Fig. 3 can be written as follows:

$$W = \{f_W\} \cdot \{\Delta\} \tag{34}$$

The tangential displacement U can be obtained,

$$U = \{f_U\} \cdot \{\Delta\} \tag{35}$$

And the sectional rotation θ can be written as:

$$\theta = \{f_\theta\} \cdot \{\Delta\} \tag{36}$$

3. Stiffness and mass matrix for the arch element

The strain energy $U_e$and, kinetic energy T_e (neglecting rotary inertia) of the arch element is given by,

$$\begin{aligned} U_e &= \frac{1}{2}\int_0^L \varepsilon^T \cdot \begin{bmatrix} EA & 0 \\ 0 & EI \end{bmatrix} \cdot \varepsilon \cdot dS \\ T_e &= \frac{1}{2}\int_0^L \rho \cdot A \cdot (\dot{U}^2 + \dot{W}^2) \cdot dS \end{aligned} \tag{37}$$

Where the dots denote the derivatives with respect to time t, ρ is the mass density of the arch material, which is considered in Ref. [16]. The Lagrangian in terms of nodal quantities can be expressed as,

$$L = T_e - U_e = \frac{1}{2}\{\dot{q}\}^T \cdot [M] \cdot \{\dot{q}\} - \frac{1}{2}\{q\} \cdot [K] \cdot \{q\} \tag{38}$$

The Euler-Lagrange equation for the curved beam under consideration become,

$$[M] \cdot \{\ddot{\Delta}\} + [K] \cdot \{\Delta\} = \{0\} \tag{39}$$

The equivalent mass matrix $[M]$ for the circular arch element , which is given by :

$$[M] = \rho \cdot A \int_v [f]^T \cdot [f] \cdot dS \tag{40}$$

Now, let us use A as the area of the section for the element, the final form of the equivalent mass matrix can be written as:

$$[M] = [M_W] + [M_U] + [M_\theta] \tag{41}$$

Where $[M]$ is defined by the relations :

$$[M_W] = \rho \cdot A \int_0^L [f_W]^T \cdot [f_W] \cdot dS \tag{42}$$

$$[M_U] = \rho \cdot A \int_0^L [f_U]^T \cdot [f_U] \cdot dS \tag{43}$$

$$[M_\theta] = \rho \cdot I \int_0^L [f_\theta]^T \cdot [f_\theta] \cdot dS \tag{44}$$

As illustrated above, the Eqs (42–44) represented the mass matrix for the radial translation$[M_W]$, the mass matrix for tangential translation $[M_U]$and lastly they represent the mass matrix for rotation $[M_\theta]$.

and, the stiffness matrix can be calculated in Eq. (38) by,

$$[K] = [T]^T \cdot \left[EI \left(\int_0^L \{H_\kappa\}^T \cdot \{H_\kappa\} dS + \alpha \int_0^L \{B_\kappa\}^T \cdot \{B_\kappa\} dS + \beta \int_0^L \{Q_\kappa\}^T \cdot \{Q_\kappa\} dS \right) \right] \cdot [T] \tag{45}$$

where

$$\{B_\kappa\} = \frac{\{\partial H_\kappa\}}{\partial S}, \quad \{Q_\kappa\} = \frac{\partial^2 \{H_\kappa\}}{\partial S^2}, \quad \beta = \tfrac{IR^2}{A}, \quad \alpha = \tfrac{EI}{GAn} \tag{46}$$

Note that as the polynomial terms are integrated in calculating the stiffness matrix, the conventional Gaussian integration scheme is applicable.

Table 1
Natural frequencies (HZ) for a circular ring computed by two present element

R/h	Mode 2			Mode 4		
	Method			Method		
	Present study	Plane stress element ANSYS	Exact (Timoshenko 1955)	Present study	Plane stress element ANSYS	Exact (Timoshenko 1955)
320	10.70	10.74	10.70	58.40	58.13	58.04
250	13.70	13.74	13.70	74.82	74.40	74.28
200	17.12	17.17	17.12	93.50	93.01	92.86
150	22.83	22.87	22.83	124.70	123.97	123.81
100	34.24	34.29	34.24	187.02	185.91	185.72
80	42.80	43.00	42.80	233.70	233.15	232.14
50	68.49	68.89	68.49	373.80	373.43	371.43
40	85.59	85.83	85.49	467.13	465.04	464.30
30	114.11	114.29	114.15	622.30	618.74	619.06
20	171.10	171.56	171.22	931.12	928.16	928.59
10	340.92	341.76	342.45	1837.97	1824.40	1857.18
5	671.52	675.67	684.89	3504.46	3460.00	3714.36

4. Determination of natural frequencies and mode shapes

The elemental stiffness matrix $[K]$ and mass matrix $[M]$ are assembled to obtain global equation of motion Eq. (39). Since the free vibration is harmonic, the displacements $\{\Delta\}$ can be written as:

$$\{\Delta\} = \{q\} \cdot e^{i\omega t} \tag{47}$$

where $\{q\}$ is a column matrix of the amplitudes of the displacements $\{\Delta\}$, (ω) is the circular frequency of vibration, and t is the time. Using the Eqs 47) in (39) and then canceling the common factor $e^{\,i\omega t}$, we obtain:

$$(-\omega^2 \cdot [M] + [K]) \cdot \{q\} = \{0\} \tag{48}$$

That can be regarded as the equation of motion for a system that is undamped and free of vibration. The Eq. (48) since it has a nonzero solution for $\{q\}$ it can be rewritten as:

$$\left|-\omega^2 \cdot [M] + [K]\right| = \{0\} \tag{49}$$

This last equation is a characteristic equation from which the natural frequencies of free vibrations can be calculated.

5. Numerical examples

To confirm the reliability of the present study, the natural frequencies of free vibration responses obtained from the new formulation of circular arch element are compared with the existing literature and those from the conventional finite straight-beam and plane stress elements, respectively.

5.1. Free vibration of a circular ring

In order to investigate the representation of in extensional flexure behavior by the finite elements, the problem of vibrations of a circular ring is chosen and discussed in the preceding section [19]. gave the exact solutions of the natural vibration of a ring shown in Fig. 4. This problem is considered by several elements in the literatures such as [12,16] recently. The information used regarding the free vibration analysis of a circular ring are: Radius of curvature R $= 12$ in $= 0.3048$ m; Cross-section A $= 0.0375$ in^2 $= 0.0009525$ m^2; Young's modulus E $= 19 \times 10^6$ lbf/ in^2 1.31×10^{11} Pa; and the material density $\rho = 0.171 \times 10^{-3}$ slug.ft/in^4 1827 kg/m^3. Only a quarter of the ring is modeled with symmetric boundary conditions as shown in Fig. 4. Two circular arch element with a subtended angle of 90° is used to predict the modes of the whole ring. Table 1 summarizes the results of the natural frequencies reasonably for two of the lowest symmetric modes of a thin circular ring with different ratio of R/h.

The frequencies are obtained from the circular arch element and the exact solutions are given by [19]. Since the ring with $R/h = 320$ is very thin, it is clear that the present curved element is free of locking. In the very thick

Table 2
Convergence study of natural frequencies (HZ) for a thin circular ring (R/h = 320)[a]

Mode no.	Element model	Number of elements on the quarter model					
		1	2	4	8	16	Exact (Timoshenko 1955)
2	QQ6	10.71	10.70	10.70			
	C-CQ3	10.83	10.77	10.70			
	Leung		10.70		10.70	10.70	10.70
	Present study	10.77	10.70				
4	QQ6	58.05	58.04				
	C-CQ3		58.51	58.29	58.05	58.04	58.04
	Leung		58.07				
	Present study	60.27	58.40				

[a] R = 12 in, E = 19e6 psi, ρ = 0.171e-3 slug.ft/in^4.

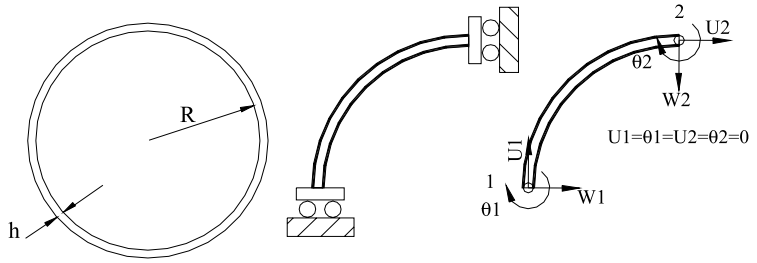

a) A pinched ring b) ¼ circular arch with nodal displacement

Fig. 4. A circular pinched ring and model for 1/4 ring.

range, shown in Table 2, a slight discrepancy is observed between analytical and finite element solutions. This is because the [19] method in the thick range is not properly applicable as the thick ring may no longer be regarded as a thin circular ring. Compared with other methods by [12,16] the solutions shows that the least mesh is required to represent the exact natural frequencies reasonably well.

5.2. Free vibration of a hinged arch

Shown in Fig. 5 is the application of the present curve beam element to the hinged circular ring with subtended angle α. The following numerical values [12] are used in this paper: Radius of curvature R = 12 in; Young's modulus E = 3.04 $\times$ 10^7 psi; Material density ρ = 0.02736 slug.ft/ in^4; t = 0.25 in; υ = 0.3 and n = 0.8497. By using the two present elements, the variation of the fundamental natural frequency (Rad/s) with subtended angle as it varies from 10° to 350°, is obtained and shown in Table 3. The solutions computed by the two present circular arch elements compared with those of [9,12] are presented in Table 3. While the results compare well with those of higher values of the angles, at lower the values there are some discrepancy. This discrepancy is due to the fact that the referred values predict a higher frequency. The displacement for the small subtended angles rises because of the beam being short in these cases making the rotary inertia and transverse shear effects important, effects that [5] did not consider but are included in the present formulation only with two elements model. It can be notice that results by [6] are obtained for 16-elements model.

5.3. Free vibration of a thick circular arch

Given by [9], the study of natural frequencies for a thick circular arch clamped at both ends are shown in Fig. 6. The following numerical values are used in this paper: Radius of curvature R = 30 in; Young's modulus E = 12 $\times$ 10^6 psi; Material density ρ = 0.283 slug.ft/in^4; υ = 0.2 and n = 0.833.

Thick circular arch is solved by three different methods shown in Table 4:

Table 3
Fundamental frequency (rad/s) values of hinged circular archs computed by two present element for various subtended angles

Angle (degrees)	Fundamental frequency (rad/s)				
	Present study	E1.1a (Krishnan et al. 1995)	E1.1b (Krishnan et al. 1995)	(Den Hartog 1928)	(Heppler 1992)
10	5862.21	5957.70	5874.30	21608.00	5849.90
20	2869.65	2826.60	2823.10	5371.10	2830.20
30	2538.53	2523.70	2345.20	2364.40	2339.70
60	569.00	562.50	561.20	561.76	560.24
90	229.50	230.65	230.40	229.95	229.77
120	115.20	116.33	116.30	115.74	115.64
150	64.14	64.96	64.93	64.48	64.44
180	37.70	38.25	38.24	37.89	37.87
210	22.66	23.06	23.05	22.78	22.77
240	13.60	13.87	13.87	13.67	13.67
270	7.89	8.06	8.06	7.93	7.93
300	4.15	4.27	4.27	4.19	4.19
330	1.69	1.73	1.73	1.69	1.69
350	0.49	0.51	0.50	0.49	0.24

Table 4
Natural frequencies (rad/s) for a thick circular arch clamped at both ends with subtended angle $\alpha = 90^\circ$

R/h	Mode 2		Mode 4	
	Method		Method	
	Present study	Plane stress element ANSYS	Present study	Plane stress element ANSYS
50	28.61	28.87	56.29	54.36
40	58.16	58.38	107.87	104.51
30	118.84	119.27	169.58	163.60
10	205.33	208.36	231.84	205.22
5	245.22	251.80	338.28	304.24
3	297.57	300.97	383.23	310.10

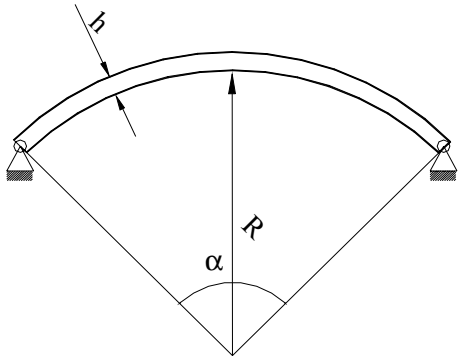

Fig. 5. A hinged circular arch with subtended angle α.

1. Using just two-element of present study.
2. Modeling the beam as a plane stress elements
3. Modeling the beam as a 20 straight beam elements [13].

The results obtained from the first method are compared to the other two methods as recorded in Table 4. While that the present curved element is free of locking. In the very thick range, a discrepancy is observed between finite element solutions. This discrepancy happens because of the straight beam element in the thick range is not properly applicable as the thick ring may no longer be regarded as a thin circular ring [13]. When the solutions are compared

Table 5
Natural frequencies (rad/s) for a quarter circular arch clamped at one end with subtended angle $\alpha = 90^{\circ}$

R/h	Mode 1		Mode 2		Mode 3	
	Method		Method		Method	
	Present study	Plane stress element ANSYS	Present study	Plane stress element ANSYS	Present study	Plane stress element ANSYS
300	0.313	0.316	1.51	1.51	4.79	4.78
200	0.469	0.472	2.266	2.274	7.19	7.17
100	0.939	0.936	4.531	4.530	14.39	14.31
50	1.877	1.884	9.057	9.110	28.88	28.71
25	3.753	3.757	18.07	18.09	58.31	56.74
12.5	7.497	7.508	35.75	35.81	117.22	110.65
6	15.52	15.54	70.97	71.19	217.76	202.26
3	30.32	30.31	120.91	122.90	278.95	262.32
1.5	55.82	55.48	163.99	174.98	310.62	298.85

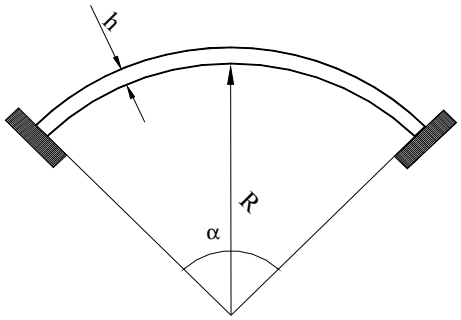

Fig. 6. A thick circular arch clamped at both ends with subtended angle α.

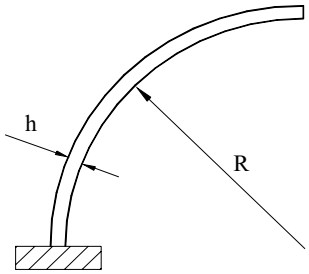

Fig. 7. A quarter ring with fixed reaction.

with the others methods, it shows that the least mesh is required to represent the exact natural frequencies reasonably well.

5.4. Free vibration of a quarter ring

Shown in Fig. 7 is a model that consists of two elements. One can make use of a program of vibration analysis with new formulation to obtain the natural frequencies and mode shapes as the ratio of thickness to length of the beam.

The following numerical values are used in this paper: Radius of curvature R = 30 in; Young's modulus E = 12 $\times$ 10^6 psi; Material density $\rho = 0.283$ slug.ft/in^4; $\upsilon = 0.2$ and $n = 0.833$. Comparing Table 5, the results of arch show good agreement with the existing finite element method.

6. Conclusions

Based on the curvature, a three nodes of the finite element model gives a satisfactory results for free vibration behavior of arches of the varied curvatures and thicknesses without locking is presented in this article; as well as, the remedy of the undesirable shear/axial locking phenomenon. The element is actually a two-node element with displacements as nodal variables when it is transformed into the final shape from a three-node element for the curvature in the beginning. The equation of motion of the element is written in final steps by Lagrangian equation. The natural frequencies and mode shapes curved structure is obtained by solving the characteristic equation of motion. To examine the convergence and accuracy of the present element, the vibration of some circular ring is analyzed by making use of two present element. A computation was carried out to study the effect of curvature and boundary conditions on the fundamental frequency of circular arches. The accuracy of element is greatly improved and the two present element can predict the lowest natural frequencies.

The results of the numerical examples shown is more accurate than other method, because it never utilizes approximation. The results are also more useful from a practical point of view to the analysis of both thin and thick curved beam. It also makes the element readily usable in the vibration analysis of curved structures, which is compatible with the existing plane stree elements.

Nomenclature

W	Radial Displacement	κ	Curvature of Element
U	Tangential Displacement	θ	Sectional Rotation
M_b	Bending moment	γ	Shearing Strain
V_b	Shearing Force	ε	Tangential Strain
N	Axial Force	n	CoeffIcient Shear
V	Nodal Curvature	$\{\Delta\}$	Nodal Displacement
$[K]$	Stiffness Matrix	ρ	Density of the Body
$[D]$	Rigidity Matrix	ω	Circular Frequency
$[M]$	Equivalent Mass Matrix	t	Time
$[f]$	Displacement Shape Functions		
E	Module of Elasticity		
I	Moment of Inertia		
A	Area of Section		
$\{q\}$	The Amplitudes of the Displacements		

References

[1] A.R. Archer, Small vibrations of incomplete circular rings, *Int J of Mech Sci* **1** (1960), 45–46.
[2] D.G. Ashwell and A.B. Sabir, Limitations of certain curved finite elements to circular arches, *Int J of Mech Eng* **13** (1971), 133–139.
[3] D.G. Ashwell, A.B. Sabir and T.M. Roberts, further studies in the application of curved finite elements to circular arches, *Int J of Mech Sci* **13** (1971), 507–517.
[4] D.J. Dawe, Numerical studies using circular arch finite elements, *Computers and Structures* **4** (1974), 729–740.
[5] J.P. Den Hartog, The lowest natural frequency of circular arcs, *Philosophical Magazine* **5** (1928), 400–408.
[6] G.R. Heppler, An element for studying the vibration of unrestrained curved Timoshenko beams, *J of Sound and Vibration* **158** (1992), 387–404.
[7] G.H. Heppler, J.S. Hansen and S. Timoshenko, beam finite elements using trigonometric basis functions, *AIAA J* **26** (1988), 1378–1388.
[8] Y. Kim and Y.Y. Kim, Analysis of thin-walled curved box beam under in-plane flexure, *J of Solids and Structures* **40** (2003), 6111–6123.
[9] A. Krishnan, S. Dharmaraj and Y.J. Suresh, Free vibration studies of arches, *J of Sound and Vibration* **186** (1995), 856–863.
[10] A. Krishnan and Y.J. Suresh, A simple cubic linear element for static and free vibration analyses of curved beams, *Computers and Structures* **68** (1998), 473–489.
[11] P.G. Lee and H.C. Sin, Locking-free curved beam element based on curvature, *Int J Numer Methods in Eng* **37** (1994), 989–1007.
[12] A.Y.T. Leung and B. Zhu, Fourier p-elements for curved beam vibrations, *Thin-walled structures* **42** (2004), 39–57.
[13] R.H. Mc Neal and R.C. Harder, *A Proposed Standard Set of Problems to Test Finite Element Accuracy*, North-Holland, 1985.
[14] S.S. Rao and V. Sundararajan, In-plane vibration of circular rings, *J Appl Mech* **36** (1969), 620–625.

[15] P. Raveendranath, G. Singh and B. Pradhan, A two-nodded locking-free shear flexible curved beam element, *Int J Numer Methods in Eng* **44** (1999), 165–280.
[16] P. Raveendranath, G. Singh and B. Pradhan, Free vibration of arches using a curved beam element based on a coupled polynomial displacement field, *Computers and Structures* **78** (2000), 583–590.
[17] A.B. Sabir and D.G. Ashwell, A comparison of curved beam elements when used in vibration problems, *J of Sound and Vibration* **18** (1971), 555–563.
[18] A. Sinaie, S.H. Mansouri, H. Saffari and R. Tabatabaei, A six node locking free curved beam element based on curvature, *Iranian Journal of Science & Technology* **27** (2003), 21–36.
[19] S. Timoshenko, *Vibration Problems in Engineering*, (3rd ed.), New York: Van Nostrand, 1955.